Research Article | Vol. 8, No. 12 | 1 Dec 2018 | OPTICAL MATERIALS EXPRESS 3761
Optical Materials EXPRESS

Spectral broadening of a single Ce^{3+}-doped garnet by chemical unit cosubstitution for near ultraviolet LED

TAO HAN,[1,*] TIANCHUN LANG,[2] YANG ZHONG,[2] SHIXIU CAO,[1] LINGLING PENG,[1] ALEKSEI YAKOVLEV,[2] AND ELENA POLISADOVA[2]

[1]*Research Institute for New Material Technology, Chongqing University of Arts and Sciences, 319 Honghe Road, Yongchuan, Chongqing 402160, China*
[2]*School of Advanced Manufacturing Technologies, National Research Tomsk Polytechnic University, 12 Timakova Street, Tomsk, 634050, Russia*
**danbaiht@126.com*

Abstract: In this paper, the isostructural $Mg_3Al_2Si_3O_{12}$ was introduced into the Ce^{3+}-doped yttrium aluminum garnet ($Y_3Al_5O_{12}$) for synthesizing $(Y_{1-x}Mg_x)_3Al_2(Al_{1-x}Si_x)_3O_{12}:Ce^{3+}$ (x = 0-0.6) solid solution phosphors. The co-substitution of the $(Mg, Si)^{6+}$ pair for the $(Y, Al)^{6+}$ pair leads to lattice shrinkage and then changes the spectral shape and width. The band peaking at ~450 nm shows a substantial broadening with the full width at half maximum increasing from 65 nm to 94 nm. The intensity of excitation spectrum (x = 0.5) at 400 nm is increased by 50% than that (x = 0). The near ultraviolet LED was fabricated with $Y_{1.5}Mg_{1.5}Al_{3.5}Si_{1.5}O_{12}:Ce^{3+}$ phosphors and a 400 nm chip and can emit strong white light. Therefore, by controlling the content of $(Y, Al)^{6+}$ substituted by $(Mg, Si)^{6+}$, the excitation spectrum of Ce^{3+}-doped $Y_3Al_5O_{12}$ can be tuned and applied for the near ultraviolet LEDs.

1. Introduction

Recently, Ce^{3+}-doped yttrium aluminum garnet ($Y_3Al_5O_{12}$) is widely applied as scintillators, afterglow materials and color converters in white light emitting diodes (WLEDs) [1,2]. The most common WLED strategy is to combine Ce^{3+}-doped $Y_3Al_5O_{12}$ phosphors and blue InGaN chips. WLED fabricated with near ultraviolet chip (300 to 410 nm) is a potential substitute for current lighting sources [3–6]. However, Ce^{3+}-doped $Y_3Al_5O_{12}$ can hardly be excited by 350-400 nm light, making it unsuitable for near ultraviolet LED. Solid solution phosphor is an efficient tool for exploring the single-activator-doped phosphors. For solid solution phosphor, the variable composition can simultaneously alter multiple parameters of the host lattice and thereby change the local environment surrounding the activator [7]. By utilizing this strategy, some novel phosphors and new luminescence phenomena have been identified, such as tunable spectrum, efficient luminous output, and improved thermal stability. Denault et al. developed $Sr_{1.975}Ce_{0.025}Ba(AlO_4F)_{1-x}(SiO_5)x$ solid solution phosphor with the maximum emission wavelength tuned from green (λ_{em} = 523 nm) to yellow (λ_{em} = 552 nm) by tuning the composition [8]. Xia et al. reported a series of solid solution phosphors such as $Ca_2(Al_{1-x}Mg_x)(Al_{1-x}Si_{1+x})O_7:Eu^{2+}$ [9] and $(CaMg)_x(NaSc)_{1-x}Si_2O_6$ [10], and provided a theoretical understanding of the tunable luminescent properties by chemical unit cosubstitution [11,12].

As a typical garnet possessing a cubic structure with Ia3d symmetry, $Mg_3Al_2Si_3O_{12}$ is isostructural with $Y_3Al_5O_{12}$, which make it possible to introduce $Mg_3Al_2Si_3O_{12}$ into Ce^{3+}-doped $Y_3Al_5O_{12}$ for forming solid solution phosphors. The introduction can be considered as $(Y, Al)^{6+}$ pair substituted by $(Mg, Si)^{6+}$ pair, which will vary the electronic and crystal structure of the host crystals, and affect the local environment surrounding Ce^{3+}. Thus, the

#345665 https://doi.org/10.1364/OME.8.003761
Journal © 2018 Received 11 Sep 2018; revised 23 Oct 2018; accepted 26 Oct 2018; published 7 Nov 2018

Optical Materials EXPRESS

excitation spectrum of the single Ce^{3+}-doped garnet is potentially anticipated to be broadened and expanded from blue light to near ultraviolet light.

In this work, $(Y_{1-x}Mg_x)_3Al_2(Al_{1-x}Si_x)_3O_{12}:Ce^{3+}$ solid solution phosphors were synthesized via introducing the isostructural $Mg_3Al_2(SiO_4)_3$ into $Y_3Al_5O_{12}:Ce^{3+}$. The anomalous spectral broadening is mainly subjected to statistical composition fluctuation because of the random distribution of Y, Mg, Al and Si at the same crystallographic site. By controlling the content of $(Y, Al)^{6+}$ substituted by $(Mg, Si)^{6+}$, the excitation spectrum of $(Y_{1-x}Mg_x)_3Al_2(Al_{1-x}Si_x)_3O_{12}:Ce^{3+}$ solid solution phosphors can be tuned to near ultraviolet region. A near ultraviolet LED fabricated with $Y_{1.5}Mg_{1.5}Al_2Al_{1.5}Si_{1.5}O_{12}:Ce^{3+}$ phosphors and a 400 nm chip can emit strong white light. This work provides a strategy for developing a near ultraviolet light phosphor from a single Ce^{3+}-doped garnet.

2. Experimental

$(Y_{1-x}Mg_x)_3Al_2(Al_{1-x}Si_x)_3O_{12}:0.06Ce^{3+}$ (x = 0-0.6) was prepared by conventional solid state reaction method. Typically, the stoichiometric amounts of Y_2O_3 (99.99%), CeO_2 (99.99%), Al_2O_3 (A. R.), SiO_2 (A. R.) and MgO (A. R.) were thoroughly mixed and then preheated at 1000°C for 2 h in air. Next, the precursors were calcined at 1600 °C for 6 h in a reductive atmosphere (H_2 10%/N_2 90%). After cooling down to room temperature, the obtained products were crushed and washed for use.

The crystal structure of samples was analyzed by X-ray diffractometer (XRD, TD-3500, Dandong, China) with Cu Kα radiation (λ = 1.5406 Å). Powder XRD data were collected in scanning mode for a 2θ range of 10-80° with a step of 0.02° and a rate of 2.0° min^{-1}. Unit cell refinements were accomplished using JADE software. The emission and excitation spectra were measured by using a fluorescent spectrophotometer (F-7000, Hitachi, Japan) with a 150 w Xe lamp as the excitation light source. The morphologies and selected area electron diffraction (SAED) images of samples were acquired using a transmission electron microscopy (TEM) and high-resolution TEM (HRTEM) analyses (JEM-21000, JEOL, Japan). The temperature quenching property was detected by thermocouples inside the plaque and was controlled with a standard high-temperature fluorescence controller (TAP-02, Orient KOJI, UK). The luminous efficiency, color-rendering index, and the Commission international de I'Eclairage (CIE) color coordinates of the fabricated LEDs were characterized using a high accuracy LED photo-color and electron test system (HSP3000, Hangzhou Hongpu Optoelectronics Technology, China) and were evaluated under a current of 350 mA.

3. Results and discussion

Figure 1(a) shows the XRD patterns of $(Y_{1-x}Mg_x)_3Al_2(Al_{1-x}Si_x)_3O_{12}:Ce^{3+}$ (x = 0-0.6). All the diffraction peaks are in agreement with the standard data of $Y_3Al_5O_{12}$ (JCPDS card No. 33-0040). No evidence of impurity was detected, indicating the solid solutions were obtained. The XRD peaks located at 33.3°correspond to (420) crystal plane and shift slightly toward the higher scattering angle with an increase of x (Fig. 1 (b)). This observation demonstrates the cosubstitution of the $(Mg, Si)^{6+}$ pair for the $(Y, Al)^{6+}$ pair changes the lattice parameters in $Y_3Al_5O_{12}$ host. As shown in Fig. 1(c), the calculated lattice constant has a decline as x increases. Hence, these results agree with the lattice shrinkage owing to replacement of Y^{3+} (0.1019 nm, CN = 8) ions in dodecahedral sites and Al^{3+} (0.039 nm, CN = 4) ions in tetrahedral sites by the smaller Mg^{2+} (0.089 nm, CN = 8) ions and Si^{4+} (0.026 nm, CN = 4) ions (Fig. 1(d)), which refer to the previous report [13].

Optical Materials EXPRESS

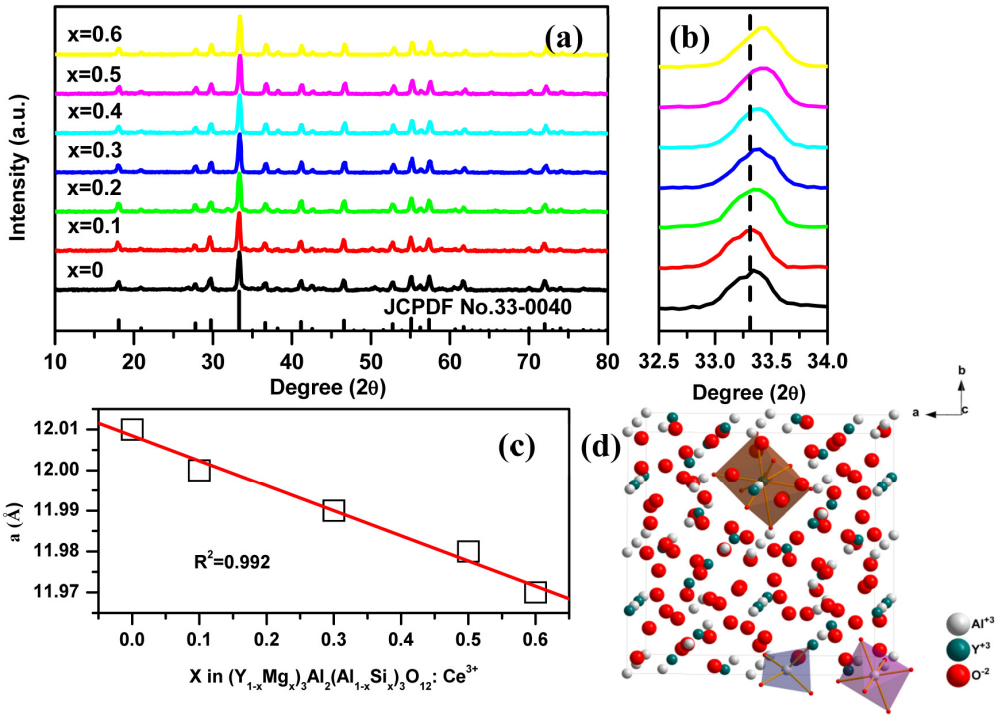

Fig. 1. (a) Full range (10-80°) XRD patterns, (b) selected diffraction peaks in the region between 32.5 and 34° and (c) lattice parameter of $(Y_{1-x}Mg_x)_3Al_2(Al_{1-x}Si_x)_3O_{12}$:0.06$Ce^{3+}$ (x = 0-0.6). (d) Crystal structures of $Y_3Al_2Al_3O_{12}$.

To confirm that the isostructural solid solution was formed, the HRTEM image and EDS mapping of a single $Y_{2.1}Mg_{0.9}Al_{4.1}Si_{0.9}O_{12}$:0.06$Ce^{3+}$ particle were measured. As shown in Fig. 2, the interplanar spacing of 0.268 nm can be assigned to the (420) crystal plane, which have decreased slightly because of lattice shrinkage. Selected-area electron diffraction pattern along a [00-1] direction shows the single crystal character of the particle. Energy-dispersive spectroscopy (EDS) mapping of a single grain shows that Al, Y, Ce, Mg and Si are homogeneous distribution in a macroscopical particle.

Optical Materials EXPRESS

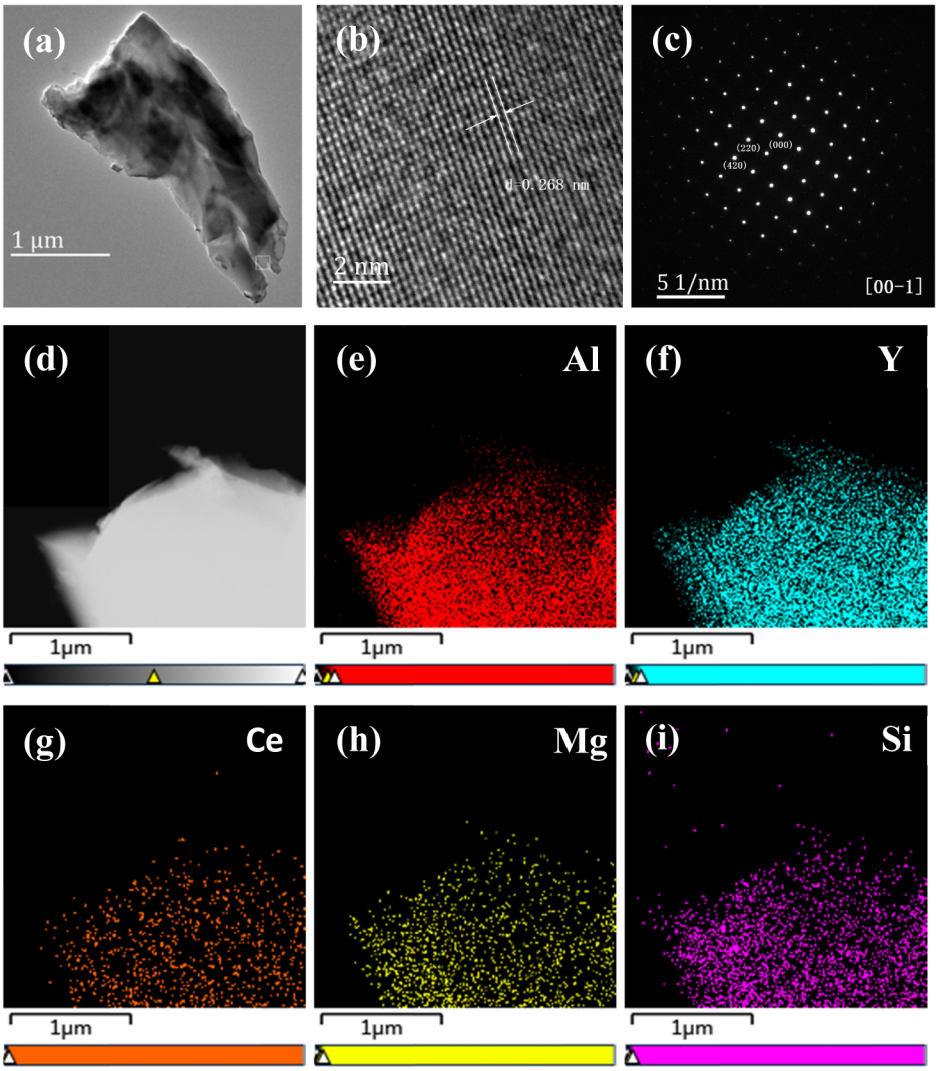

Fig. 2. (a) TEM image and (b) HRTEM image of a single $Y_{2.1}Mg_{0.9}Al_{4.1}Si_{0.9}O_{12}$:0.06$Ce^{3+}$ particle. (c) Selected-area electron diffraction pattern along a [00-1] direction. EDS mapping of (d) a single $Y_{2.1}Mg_{0.9}Al_{4.1}Si_{0.9}O_{12}$:0.06$Ce^{3}$ particle for (e) Al, (f) Y, (g) Ce, (h) Mg and (i) Si elements.

Figures 3(a) and 3(b) show excitation spectra and emission spectra of $(Y_{1-x}Mg_x)_3Al_2(Al_{1-x}Si_x)_3O_{12}$: Ce^{3+} (x = 0-0.6). Under 530 nm emission, the excitation spectra are composed of two broad bands with the peaks at ~340 nm and ~450 nm, corresponding to the 5d–4f electronic excitation of Ce^{3+}. With increasing x, the two bands show a distinct broadening. In particular for the band peaking at ~450 nm which is suitable for blue LED chips, its left wing is obviously raised and blue-shifted, whereas the right wing is slightly red-shifted. The full width at half maximum (FWHM) increases monotonically from 65 nm (x = 0) to 94 nm (x = 0.6), containing 23 nm blue-shift of left wing and 6 nm red-shift of right wing. The anomalous spectral broadening can be attributed to reduced structure symmetry, enhanced structural disorder and statistical composition fluctuation caused by the random distribution of Y, Mg, Al and Si at the same crystallographic sites [14]. The change of spectral width is dependent on evolution of the local environment surrounding Ce^{3+} in $Y_3Al_5O_{12}$.

Optical Materials EXPRESS

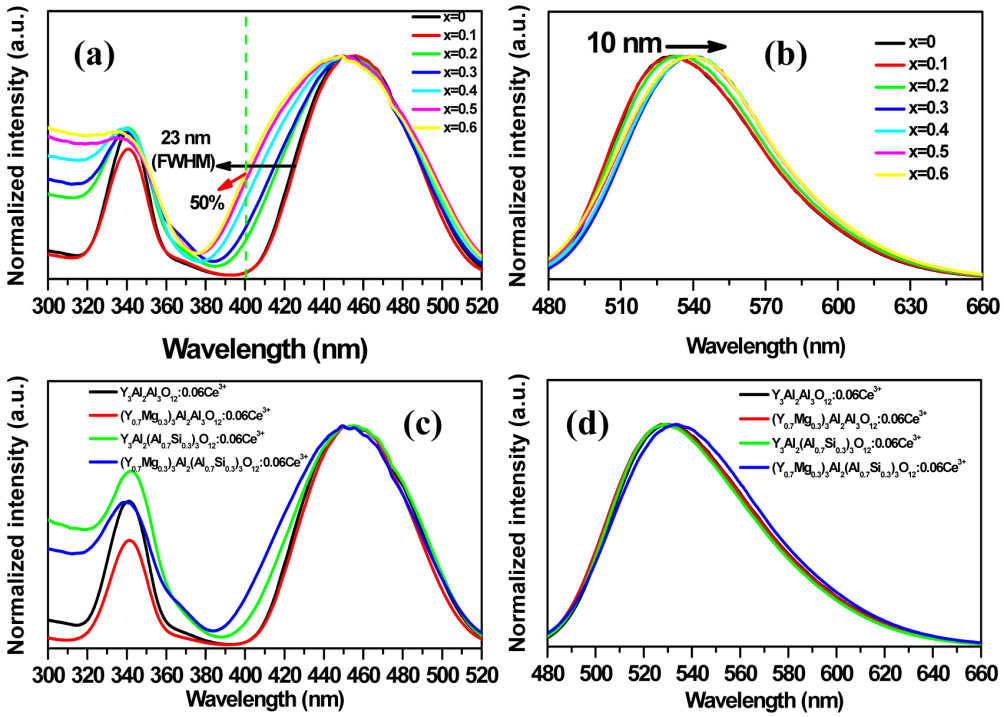

Fig. 3. (a) Normalized excitation spectra and (b) emission spectra of $(Y_{1-x}Mg_x)_3Al_2(Al_{1-x}Si_x)_3O_{12}$:0.06$Ce^{3+}$ (x = 0-0.6). (c) Excitation spectra and (d) emission spectra of $Y_3Al_5O_{12}$:0.06Ce^{3+} with doping different elements (Mg^{2+}, Si^{4+}, and (Mg, Si)$^{6+}$).

Figures 4(b) and 4(c) show a CeO_8 polyhedron is simultaneously coordinated by six $(Al/Si)O_4$ tetrahedra through nodes and edges, and by four $(Mg/Y)O_8$ square antiprisms through edges [15]. With varying x, the evolution of local environment surrounding Ce^{3+} from Al-rich site to Si-rich site and Y-rich site to Mg-rich site because of introducing $Mg_3Al_3Si_2O_{12}$ (Figs. 4(a) and 4(d)). The variation of the Si/Al and Mg/Y ratios play crucial roles in the change of the spectral shape and the spectral width. Analyzed via Gaussian fitting (Figs. 4(e)-4(g)), the band peaking at ~450 nm was divided into three sub-bands peaking at ~413 nm (Ce(I)), ~450 nm (Ce(II)) and ~488 nm (Ce(III)), respectively. Considering Si/Al ratio has a more important effect on the spectral width than that of Mg/Y ratio (Fig. 3(c)), Ce(I) is believed to reside at a Si-rich site, whereas Ce(II) resides at an Al-rich site; Ce(III) is believed to reside at a Mg-rich site, whereas Ce(II) resides at an Y-rich site. When x = 0.3, 0.4 and 0.5, the luminescence intensity ratios of Ce(I)/Ce(II)/Ce(III) are 0.09/0.96/0.20, 0.13/0.96/0.23 and 0.36/0.95/0.25, respectively, which well match with the sharply enhanced left wing and slightly enhanced right wing, that can be contributed to broadened excitation spectra.

Optical Materials EXPRESS

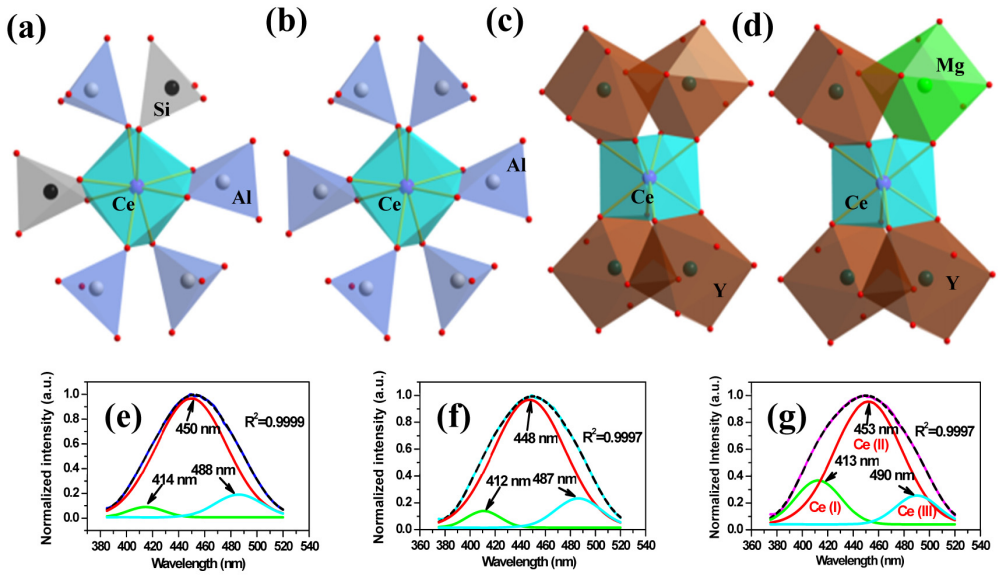

Fig. 4. Local environment of CeO_8 surrounded by $(Si/Al)O_4$ (a), AlO_4 (b), YO_8 (c), and $(Mg/Y)O_8$ (d)in the crystal structure. Gaussian fitting of the excitation spectra of $(Y_{1-x}Mg_x)_3Al_2(Al_{1-x}Si_x)_3O_{12}$: Ce^{3+} with x = 0.3 (e), 0.4 (f) and 0.6 (g)

In addition to the excitation spectral broadening, the red-shift of emission spectra is also an interesting feature of the solid solution phosphors. The peak emission is red-shifted by 10 nm, moving from 530 nm (x = 0) to 540 nm (x = 0.60). Owing to the substitution of Mg for Y and Si for Al, the decrease of structure symmetry and the lattice shrinkage, and self-absorption increase usually induce to yield large crystal field splitting which red-shift the photoluminescence spectra. However, Fig. 3(c) and d show the excitation spectral broadening is weakened and emission spectra have no obvious shift, as the single substitution of Mg for Y, or Si for Al in host lattice. During the process of doping Mg^{2+} or Si^{4+} into the $Y_3Al_5O_{12}$ lattice, cation vacancies and oxygen vacancies will appear. These vacancies, namely crystal lattice defects, increase the probability of non-radiative transitions, and thus decrease Ce (I) or Ce (III) luminescent efficiency, which may reduce the excitation spectral broadening and spectral shift [16].

The thermal stability, which will induce luminescence quenching or even degradation of phosphors, plays an important role for the application. Figure 5 shows the temperature-dependence of the photoluminescence properties of the synthesized $(Y_{1-x}Mg_x)_3Al_2(Al_{1-x}Si_x)_3O_{12}$:0.06$Ce^{3+}$ (x = 0-0.4). The relative photoluminescence intensity of the sample decreases with increasing temperature over the range of 25 to 250 °C due to the larger nonradiative transition probability at higher temperatures. The thermal quenching is reduced and then progressively increased with increasing x. At 140 °C (413 K), the emission intensity is reduced by 20%, 17%, 24%, 29%, 31% for x = 0-0.4. Of these, $Lu_{2.7}Mg_{0.3}Al_{4.7}Si_{0.3}O_{12}$:$Ce^{3+}$ exhibits the best thermal ability of emission. The electron density around O^{2-} anions is essentially competed by activator ion and the neighboring cations, so the M-O^{2-} (M = Mg^{2+}, Si^{4+}, Y^{3+}, and Al^{3+}) bonding will mainly control the degree of covalence in the Ce^{3+}–O^{2-} bonding. Compared with the larger $(Y, Al)^{6+}$ pairs, the bonds connecting between smaller (Mg, Si) $^{6+}$ pairs and O^{2-} anions are relatively covalent, so the covalence of Ce^{3+}–O^{2-} bonds is weakened. Herein, the Ce^{3+}–O^{2-} bonds become less covalent as x increases. The covalence of Ce^{3+}–O^{2-} bond is progressively decreased by the neighbor cation control, resulting in the reduction of the thermal quenching activation energy [17].

Optical Materials EXPRESS

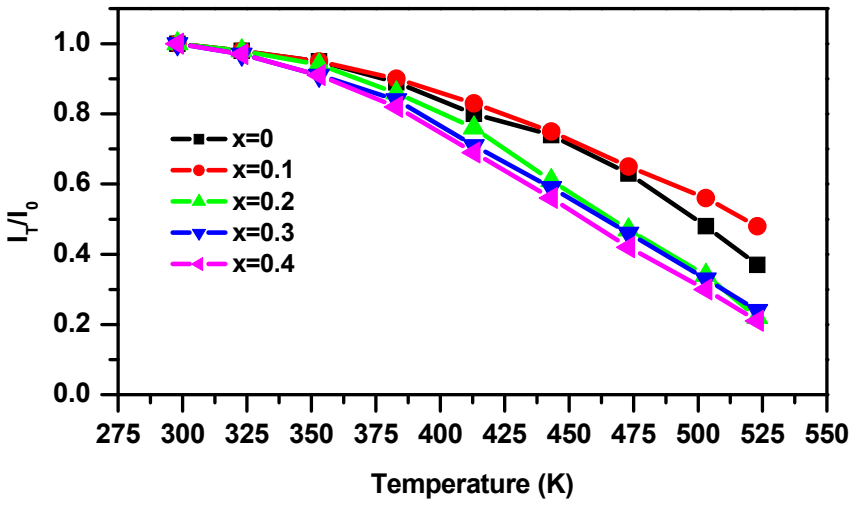

Fig. 5. Temperature-dependent emission intensity of $(Lu_{1-x}Mg_x)_3Al_2(Al_{1-x}Si_x)_3O_{12}:Ce^{3+}$ (x = 0-0.4).

In this work, $(Y_{1-x}Mg_x)_3Al_2(Al_{1-x}Si_x)_3O_{12}:0.06Ce^{3+}$ solid solution phosphors exhibit broadened excitation spectra and red-shifted emission spectra. The obtained phosphors can suit well not only the blue chips but also near ultraviolet chips. As mentioned in Fig. 3(c), compared with x = 0, as x = 0.5 the excitation intensity remarkably rises by 50%. Two LEDs were fabricated with $Y_{1.5}Mg_{1.5}Al_{3.5}Si_{1.5}O_{12}$: Ce^{3+} phosphors by using 450 nm and 400 nm chips, respectively (Fig. 6). The chromaticity coordinate of the LEDs fabricated with 450 nm and 400 nm chips are (x = 0.2843 y = 0.2687) and (x = 0.3771 y = 0.4356), respectively. The luminous efficacies of these LEDs are 103.9 and 55.5 lm/W under 350-mA drive current. It is very interesting to find that the luminous efficacies are well consistent with the excitation intensity at different wavelength. These findings show this series of phosphors can promote application in white light-emitting diodes.

Optical Materials EXPRESS

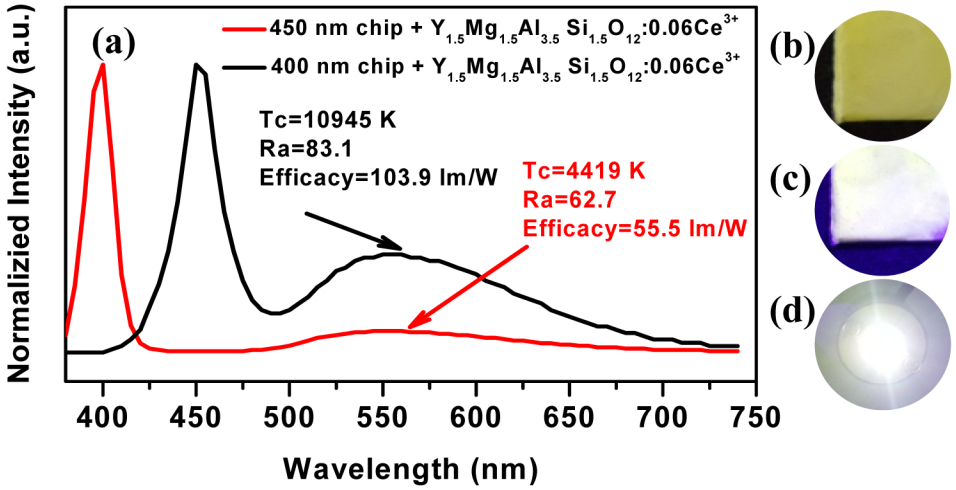

Fig. 6. (a) Electroluminescence spectra of wLEDs fabricated with different chips and $(Y_{1-x}Mg_x)_3Al_2(Al_{1-x}Si_x)_3O_{12}$: Ce^{3+} phosphors. Images of $Y_{1.5}Mg_{1.5}Al_{3.5}Si_{1.5}O_{12}$:$Ce^{3+}$ under (b) natural light and (c) 400 nm light. (d) Image of a wLED using 400 nm chip driven under 350 mA.

4. Conclusions

In conclusion, the $(Y_{1-x}Mg_x)_3Al_2(Al_{1-x}Si_x)_3O_{12}$:$Ce^{3+}$ solid solution phosphors were synthesized by conventional solid state reaction method. The obtained particle shows the single crystal character and the cations (Al, Y, Ce, Mg and Si) are homogeneous distribution. With increasing x, the band peaking at ~450 nm has a distinct broadening and the FWHM increases monotonically from 65 nm (x = 0) to 94 nm (x = 0.6). The cosubstitution of the $(Mg, Si)^{6+}$ pair for the $(Y, Al)^{6+}$ pair causes lattice shrinkage and changes the spectral shape width. The band with the peak of ~450 nm can be divided into three sub-bands peaking at ~413 nm (Ce(I)), ~450 nm (Ce(II)) and ~488 nm (Ce(III)), respectively. When x = 0.3, 0.4 and 0.5, the luminescence intensity ratio of Ce (I)/Ce (II)/Ce (III) is 0.09/0.96/0.20, 0.13/0.96/0.23 and 0.36/0.95/0.25, respectively, which is well consistent with the definitely enhanced left wing and slightly enhanced right wing. The intensity of excitation light (x = 0.5) is enhanced by 50% at 400 nm compared with x = 0. The luminous efficacies of the LEDs using 450 nm and 400 nm LED chips are 103.9 and 55.5 lm/W under 350-mA drive current. The broadened excitation spectrum of the obtained solid solution phosphors will extend the applied range from blue light to near ultraviolet light in white light-emitting diodes.

Funding

Natural Science Foundation of Chongqing (cstc2018jcyjAX0339, cstc2016jcyjA0567, cstc2017jcyjAX0393); Chongqing Youth Science and Technology Talent Cultivation Project (cstc2014kjrc-qnrc40006); Chongqing International Science & Technology Cooperation Program (cstc2015gjhz0003).

References

1. Z. Xia and A. Meijerink, "Ce^{3+}-Doped garnet phosphors: composition modification, luminescence properties and applications," Chem. Soc. Rev. **46**(1), 275–299 (2017).
2. Z. Xia and Q. Liu, "Progress in discovery and structural design of color conversion phosphors for LEDs," Prog. Mater. Sci. **84**, 59–117 (2016).
3. S. Pimputkar, J. S. Speck, S. P. DenBaars, and S. Nakamura, "Prospects for LED lighting," Nat. Photonics **3**(4), 180–182 (2009).
4. C. C. Lin, Y. P. Liu, Z. R. Xiao, Y. K. Wang, B. M. Cheng, and R. S. Liu, "All-in-one light-tunable borated phosphors with chemical and luminescence dynamical control resolution," ACS Appl. Mater. Interfaces **6**(12), 9160–9172 (2014).

Optical Materials EXPRESS

5. A. Huang, Z. Yang, C. Yu, Z. Chai, J. Qiu, and Z. Song, "Tunable and white light emission of a single-phased $Ba_2Y(BO_3)_2Cl:Bi^{3+}$, Eu^{3+} phosphor by energy transfer for ultraviolet converted white LEDs," J. Phys. Chem. C **121**(9), 5267–5276 (2017).
6. J. Zhao, Z. Yang, C. Yu, J. Qiu, and Z. Song, "Preparation of ultra-small molecule-like Ag nano-clusters in silicate glass based on ion-exchange process: energy transfer investigation from molecule-like Ag nano-clusters to Eu^{3+} ions," Chem. Eng. J. **341**, 175–186 (2018).
7. W. B. Im, N. George, J. Kurzman, S. Brinkley, A. Mikhailovsky, J. Hu, B. F. Chmelka, S. P. DenBaars, and R. Seshadri, "Efficient and color-tunable oxyfluoride solid solution phosphors for solid-state white lighting," Adv. Mater. **23**(20), 2300–2305 (2011).
8. K. A. Denault, N. C. Georege, S. R. Paden, S. Brinkley, A. A. Mikhailovsky, J. Neuefeind, S. P. DenBaars, and R. A. Seshadri, "A green-yellow emitting oxyfluoride solid-solution phosphor $Sr_2Ba(AlO_4F)_{1-x}(SiO_5)_x:Ce^{3+}$ for thermally stable, high color rendition solid state white lighting," J. Mater. Chem. **22**(35), 18204–18213 (2012).
9. Z. Xia, C. Ma, M. S. Molokeev, Q. Liu, K. Rickert, and K. R. Poeppelmeier, "chemical unit cosubstitution and tuning of photoluminescence in the $Ca_2(Al_{1-x}Mg_x)(Al_{1-x}Si_{1+x})O_7:Eu^{2+}$ phosphor," J. Am. Chem. Soc. **137**(39), 12494–12497 (2015).
10. Z. Xia, G. Liu, J. Wen, Z. Mei, M. Balasubramanian, M. S. Molokeev, L. Peng, L. Gu, D. J. Miller, Q. Liu, and K. R. Poeppelmeier, "Tuning of photoluminescence by cation nanosegregation in the $(CaMg)_x(NaSc)_{1-x}Si_2O_6$ solid solution," J. Am. Chem. Soc. **138**(4), 1158–1161 (2016).
11. J. Qiao, L. Ning, M. S. Molokeev, Y.-C. Chuang, Q. Liu, and Z. Xia, "Eu^{2+} site preferences in the mixed cation $K_2BaCa(PO_4)_2$ and thermally stable luminescence," J. Am. Chem. Soc. **140**(30), 9730–9736 (2018).
12. J. Qiao, Z. Xia, Z. Zhang, B. Hu, and Q. Liu, "Near UV-pumped yellow-emitting $Sr_9MgLi(PO_4)_7:Eu^{2+}$ phosphor for white-light LEDs," Sci. China Mater. **61**(7), 985–992 (2018).
13. Y. Jia, Y. Huang, Y. Zheng, N. Guo, H. Qiao, Q. Zhao, W. Lv, and H. You, "Color point tuning of $Y_3Al_5O_{12}:Ce^{3+}$ phosphor via Mn^{2+}–Si^{4+} incorporation for white light generation," J. Mater. Chem. **22**(30), 15146–15152 (2012).
14. L. Wang, R. J. Xie, Y. Li, X. Wang, C. G. Ma, D. Luo, T. Takeda, Y. T. Tsai, R. S. Liu, and N. Hirosaki, "$Ca_{1-x}Li_xAl_{1-x}Si_{1+x}N_3:Eu^{2+}$ solid solutions as broadband, color-tunable and thermally robust red phosphors for superior color rendition white light-emitting diodes," Light Sci. Appl. **5**(10), e16155 (2016).
15. H. Ji, L. Wang, M. S. Molokeev, N. Hirosaki, Z. Huang, Z. Xia, O. M. Kate, L. Liu, and R. J. Xie, "New garnet structure phosphors, $Lu_{3x}Y_xMgAl_3SiO_{12}$: Ce^{3+} (x = 0–3), developed by solid solution design," J. Mater. Chem. C Mater. Opt. Electron. Devices **4**(12), 2359–2366 (2016).
16. G. Li and J. Lin, "Recent progress in low-voltage cathodoluminescent materials: synthesis, improvement and emission properties," Chem. Soc. Rev. **43**(20), 7099–7131 (2014).
17. W. Y. Huang, F. Yoshimura, K. Ueda, Y. Shimomura, H. S. Sheu, T. S. Chan, C. Y. Chiang, W. Zhou, and R. S. Liu, "Chemical pressure control for photoluminescence of $MSiAl_2O_3N_2:Ce^{3+}/Eu^{2+}$ (M = Sr, Ba) oxynitride phosphors," Chem. Mater. **26**(6), 2075–2085 (2014).